Methylenebis(*p*-phenyl isocyanate)-Based Polyurethane Ionomers. 2. Structure–Property Relationships

Day-chyuan Lee,[‡] Richard A. Register, Chang-zheng Yang,[†] and Stuart L. Cooper*

Department of Chemical Engineering, University of Wisconsin—Madison, Madison, Wisconsin 53706. *Received July 28, 1987*

ABSTRACT: The effects of polyol molecular weight and ionization level on the properties of elastomeric polyurethane ionomers were studied. The rubbery plateau modulus was found to depend on the fraction of ionic groups in the material. For the unionized polyurethane, the glass transition temperature of the copolymer was adequately described by the Fox equation. As the ionization level increased, the matrix T_g dropped due to aggregation of the ionized MDI units. Wide-angle X-ray scattering revealed no stress-induced crystallization in an ionomer prepared from a short-chain poly(tetramethylene oxide) polyol. A new morphological model is applied to small-angle X-ray scattering data and the results are compared with the physical property trends.

Introduction

Ionomers are copolymers typically containing less than 10% acid comonomer. These materials are often elastomers over some range of temperature, with aggregates of ionic groups acting as physical cross-links. Ionomer properties depend strongly on the type of polymer backbone and types and amounts of acid functionality and neutralizing cation.[1] Considerable effort has been directed at understanding the structure–property relationships of ionomers.[2] Most of these studies have been carried out on systems consisting of a hydrophobic monomer randomly copolymerized with a minor amount of carboxylate- or sulfonate-containing comonomer. We have recently synthesized polyurethane model ionomers which have a well-defined topological spacing between ionic groups.[3] These materials were studied with small-angle X-ray scattering (SAXS) and a new morphological model was proposed to rationalize the two small-angle peaks observed. This model is based on a liquidlike dispersion of bead–spring micronetworks and incorporates as parameters the ionic multiplet radius, the distance between the multiplets, the average cross-link functionality of the multiplets, and the radius and volume fraction of the bead–spring micronetworks in the material. In this paper, the effects of ionization level and polyol molecular weight on the properties of these polyurethane ionomers are examined.

Experimental Section

A. Sample Preparation. The synthetic method used to prepare the polyurethane ionomers has been described in the first paper of this series.[3] The polyols used were poly(tetramethylene oxide) (PTMO, M_n = 668 (Polysciences), 970, 2039 (Quaker Oats Co.), and 2900 (Du Pont)). These polyols were reacted with methylenebis(*p*-phenyl isocyanate), MDI (Eastman Kodak), sodium hydride (NaH, Aldrich), and γ-propane sultone (Aldrich). The chemical structure of the polymers studied is shown in Figure 1. The values of X in Figure 1 are approximately 9, 13, 28, and 40, respectively, for the different polyol molecular weights. The polystyrene-equivalent number-average molecular weight of the base polyurethane, as determined by gel-permeation chromatography, exceeded 20 000 in all cases.

The ionization level of each sample was verified by elemental analysis for sodium; the sodium contents are listed in Table I. In the mnemonic sample code used throughout this paper, the first letter refers to the polyol type ("M" for PTMO), the first number is the polyol molecular weight in thousands, the next two letters are the cation's chemical symbol ("Na" for sodium), and the two-digit number at the end is the percentage ionization of the material. The percent of urethane hydrogens replaced, or ionization level, was calculated from the known composition of the base polyurethane and the measured sodium contents. Although it was intended to prepare a fully ionized ionomer for each polyol molecular weight, this condition was difficult to achieve for polymers incorporating low molecular weight PTMO due to poor mixing of the NaH in the polymer solution.

Table I
Sample Designations, Compositions, and Thermal Properties

sample	wt % Na	T_g, °C (DSC)	T_g, °C (E'' peak)	T_m, °C (DSC)	ΔH, cal/g
M.7Na.73	2.96	−52	−50		
M.7Na.39	1.74	−41	−38		
M.7Na.25	1.15	−38	−37		
M.7Na.00	0	−33			
M1Na.81	2.55	−71	−68		
M1Na.49	1.64	−64	−62		
M1Na.36	1.24	−61	−60		
M1Na.00	0	−55			
M2Na.99	1.77	−78	−76	0	
M2Na.71	1.30	−75	−73	4	0.45
M2Na.35	0.67	−72	−71	16	10.70
M2Na.00	0	−68		25	13.20
M3Na.96	1.29	−78	−76	9	1.69
M3Na.00	0	−72		28	17.45

Samples for SAXS, mechanical testing, and thermal analysis were spin-cast from *N,N*-dimethylformamide (Aldrich), dried in a vacuum oven at 60 °C for 1 week, and then stored in a desiccator at room temperature until studied.

B. Experimental Procedures. Dynamic mechanical data were collected at 110 Hz by using a computer-controlled Toyo Rheovibron DDV-IIC. Film samples, about 0.04 × 3 × 20 mm in size, were tested under a nitrogen blanket from −150 to 200 °C at a heating rate of 2 °C/min. DSC thermograms over the temperature range from −120 to 250 °C were recorded on a Perkin-Elmer DSC-II interfaced with a thermal analysis data station (TADS). The experiments were carried out at a heating rate of 20 °C/min under helium purge on samples weighing 16 ± 2 mg. Calibration was done by using indium and mercury. A scanning autozero module was used to minimize instrumental nonlinearity over the temperature range of interest. Uniaxial stress–strain measurements were made at room temperature by using an Instron TM with a crosshead speed of 0.5 in./min. Dumbbell-shaped film samples were stamped out with an ASTM D1708 die. Reported data are the average of three tests. The SAXS procedures and instrumentation have been described previously.[3] The wide-angle X-ray scattering (WAXS) experiments were performed at the Cornell High-Energy Synchrotron Source (CHESS). An X-ray energy of 8042 eV (Cu Kα) was used, with the X-rays collimated into a square measuring 1.0 × 1.0 mm. Polaroid Type 52 film was used, with a sample-to-film distance of 40 mm. The ionomer samples used were the same as those used for the SAXS measurements, and the samples were held in a

* To whom correspondence should be addressed.
† Present address: Department of Chemistry, Nanking University, People's Republic of China.
‡ Present address: Exxon Research and Engineering, Annandale, NJ 08801.

0024-9297/88/2221-1005$01.50/0

Table II
Tensile Properties

sample	plateau modulus at 50 °C, MPa	plateau region, °C onset	plateau region, °C end	E_{100}[a](25 °C), MPa	stress at break (25 °C), MPa	elongation at break (25 °C), %
M.7Na.73	144.1	0	170	22.9	36.7	340
M.7Na.39	27.1	10	140	12.4	43.0	430
M.7Na.25	11.7	20	120	8.0	40.7	510
M1Na.81	101.9	0	150	12.0	26.1	600
M1Na.49	20.3	10	140	6.8	29.0	770
M1Na.36	13.8	10	130	4.7	23.2	860
M2Na.99	28.5	0	140	6.4	33.7	940
M2Na.71	18.8	10	130	4.9	26.0	940
M2Na.35	5.9	40	110	1.8	17.6	1110
M3Na.96	17.7	10	130	2.3	7.7	1200

[a] Secant modulus at 100% elongation.

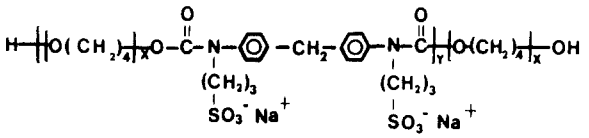

Figure 1. Chain architecture of model polyurethane ionomers based on PTMO.

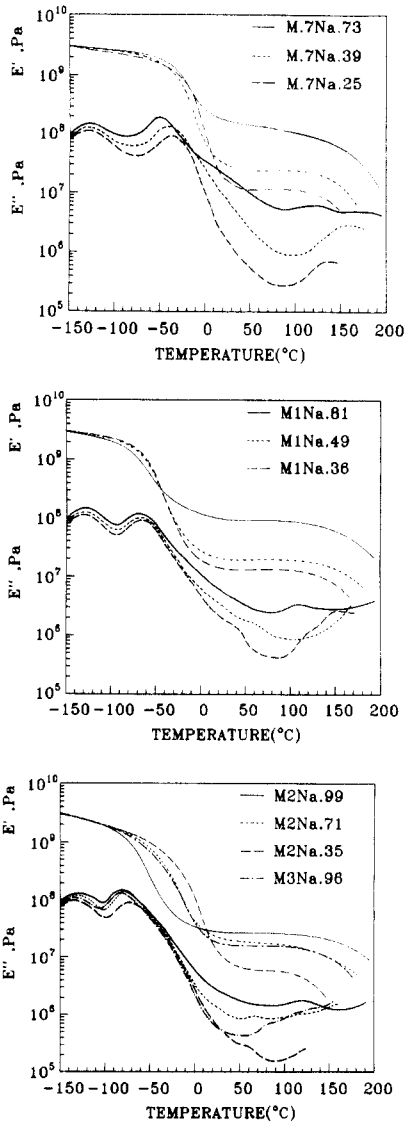

Figure 2. Dynamic mechanical results (110 Hz) for the sulfonated PTMO–MDI polyurethane ionomers: (top) PTMO 668; (middle) PTMO 970; (bottom) PTMO 2039, 2900.

stretching jig which allowed continuous elongation of the specimen. The samples were stretched and allowed to relax for a minimum of 30 min before WAXS photographs were taken.

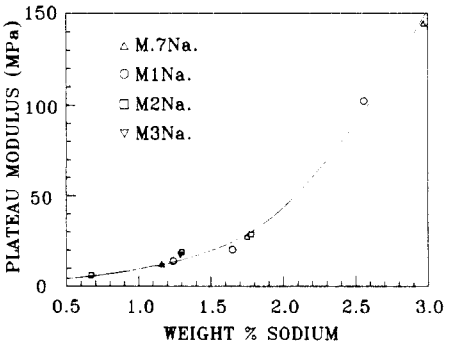

Figure 3. Correlation between plateau modulus and ion content.

Results and Discussion

A. Dynamic Mechanical Analysis. Figure 2 shows the dynamic mechanical responses of these ionomers, while Table II lists the plateau moduli (determined at 50 °C) and approximate plateau widths. The plateau modulus increases with ionization level. Since the ionic groups aggregate to form physical cross-links, as the ionization level increases, so does the cross-link density, which raises the modulus. Also, the breadth of the plateau region increases with ionization level. The onset of the rubbery plateau occurs at progressively lower temperatures as the ionization level is increased, because the ionized MDI units form microdomains within the material, enriching the matrix in the lower T_g PTMO. Also, the upper temperature limit of the plateau modulus increases with ionization level, indicating that the ionic cross-links remain stable to higher temperatures.

The E'' curves in Figure 2 show small maxima in the 50–100 °C range, with the temperature of the maximum decreasing with ionization level. We presently have no explanation for the origin of these loss peaks, although the strong correlation with ionization level indicates they are not artifacts.

The plateau modulus is plotted versus weight percent sodium in Figure 3. Note that the average molecular weight between cross-links is inversely proportional to the weight percent sodium. The superposition of data from ionomers with different polyol molecular weights onto a single curve (drawn as an aid to the eye only) indicates that the ion content is the single variable controlling the plateau modulus. This result agrees with the concept of ionic aggregates acting as physical cross-links.

B. DSC Results. DSC curves for the polyurethane ionomers based on PTMO 2039 are shown in Figure 4. Results for the other materials were similar. Three general features are observable in the DSC traces. The matrix glass transitions fall in the range −30 to −80 °C for all samples. Since the matrix is primarily PTMO, this corresponds roughly to a PTMO glass transition. For ion-

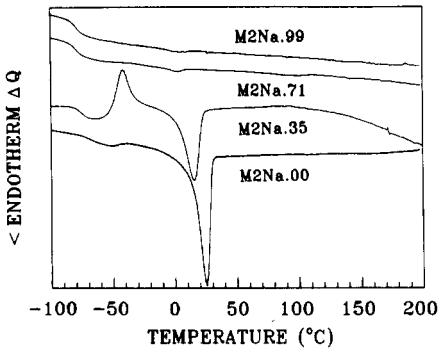

Figure 4. DSC traces for materials based on PTMO 2039.

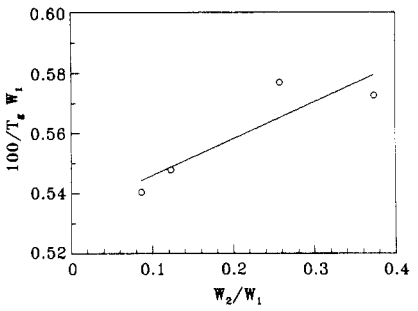

Figure 5. Plot of DSC data for unionized polyurethanes according to the Fox equation (1 = PTMO, 2 = MDI).

omers based on polyols of 2039 and 2900 molecular weight, a PTMO melting endotherm is visible near 25 °C. The small exotherm visible in the M2Na.35 and M2Na.00 samples near −40 °C is the result of PTMO crystallization in the temperature region between the PTMO glass transition and melting point.

The transition temperatures obtained from the DSC measurements are listed in Table I. The glass transition temperatures agree within 3 °C with the peaks of the E'' curves determined by dynamic mechanical analysis at 110 Hz, also listed in Table I. The unionized materials exhibit a sharp glass transition zone, characteristic of one-phase materials. As these are strictly 1:1 copolymers, lowering the polyol molecular weight increases the weight fraction of MDI in the material. The Fox equation[4] is often used to describe the glass transition behavior of single-phase copolymers:

$$1/T_g = W_1/T_{g1} + W_2/T_{g2} \quad (1)$$

which may be rewritten as

$$1/T_g W_1 = 1/T_{g1} + (W_2/W_1)/T_{g2} \quad (2)$$

W_1 and W_2 are the weight fractions of components 1 and 2; T_g, T_{g1}, and T_{g2} are the glass transition temperatures for the copolymer and homopolymers 1 and 2. Considering component 1 to be PTMO and component 2 to be MDI, Figure 5 shows a plot of the data in the form of eq 2. Although some scatter is clearly present, a best fit of the data to eq 2 gives a value of −86 °C for the PTMO glass transition, which is close to the literature value[5] of −84 °C.

For the ionomers, the values in Table III show that increasing the ion content lowers the glass transition temperature. This trend parallels that found by dynamical mechanical analysis, where the rubbery plateau was found to begin at progressively lower temperatures as the ionization level increased. As more MDI units are ionized, they microphase-separate into aggregates, enriching the matrix in the lower T_g PTMO.

The behavior of the PTMO melting peak as the ionization level changes also reflects the process of ionic aggregation. A large peak is observed for the unionized

Table III
SAXS Modeling Results

sample	R_1, nm	D, nm	R_{CA}, nm	V_f
M.7Na.73	0.80	2.23	2.80	0.39
M.7Na.39	0.82	2.12	2.85	0.35
M.7Na.25	0.84	1.97	2.89	0.27
M1Na.81	0.81	2.53	3.09	0.35
M1Na.49	0.83	2.08	3.10	0.33
M1Na.36	0.85	2.03	3.29	0.30
M2Na.99	0.85	2.76	3.08	0.27
M2Na.71	0.89	2.42	3.16	0.25
M2Na.35	0.97	2.35	3.36	0.14
M3Na.96	0.91	2.65	4.03	0.24

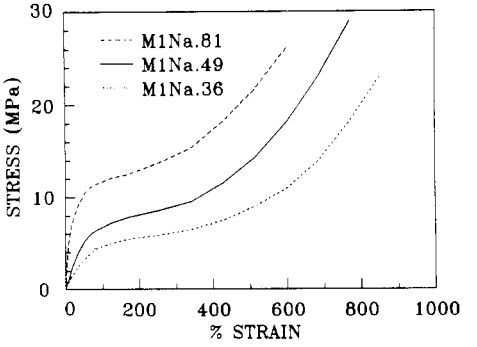

Figure 6. Stress–strain curves at 25 °C for materials based on PTMO 970.

materials, but as the ionization level increases, this peak decreases in area and shifts to lower temperatures. The T_m and ΔH values are listed in Table III. It is possible that, in the unionized material, the single MDI unit acts as a crystal defect but does not limit the size of the PTMO crystallites. In the ionized materials, the PTMO cannot crystallize around an ionic aggregate; thus, the PTMO crystallites must be smaller than in the unionized material, and melt at a lower temperature. Also, the fraction of PTMO incorporated into crystals is reduced, resulting in a smaller melting endotherm. A similar phenomenon has been proposed for ethylene/methacrylic acid ionomers,[6] where the size of the ethylene lamellae is governed by the spacing between "ionic pockets".

C. Stress–Strain Analysis. Figure 6 shows stress–strain curves for the ionomer based on PTMO 970; the curves of the other ionomers are similar. The tensile parameters determined from the curves are summarized in Table II. The modulus of these ionomers increases with increasing ionization level and decreases with PTMO molecular weight, as was found by dynamic mechanical testing. Also, the elongation at break increases with PTMO molecular weight and decreases with ionization level. Such behavior is expected based on the extensibility of the segments between ionic aggregates. As unionized MDI units remain dispersed in the matrix, decreasing the ionization level will increase the average topological distance between ionic aggregates, which has the same effect as lengthening the PTMO segments.

The enhancement of the strength at large elongation is often ascribed to either strain-induced crystallization[12,13] or the finite extensibility of the polymer chains. Strain-induced crystallization in polyurethane[14] and poly(urethane–urea)[15] block copolymers has been observed by wide-angle X-ray scattering (WAXS) to begin at extensions as low as 150% for materials based on PTMO 2000. Thus, it seemed likely that stress-induced crystallization was present in these ionomers as well. To test this hypothesis, we performed WAXS studies on the M.7Na.25 material. At 700% elongation, this sample showed the WAXS pattern in Figure 7. The amorphous halo shown has an

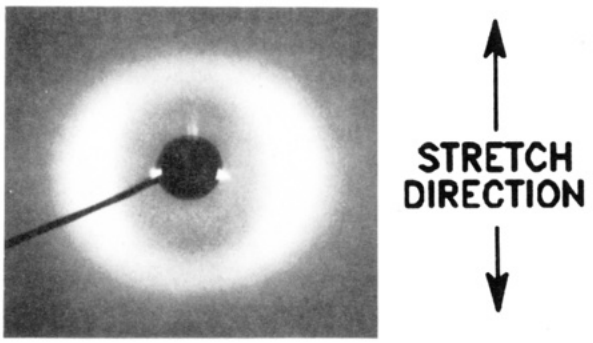

Figure 7. WAXS pattern for sample M.7Na.25 at 700% elongation. Stretch direction is as indicated. Intensity spots at the beam stop are artifactual.

average Bragg spacing of 4.54 ± 0.08 Å, which corresponds well to the value of 4.5 Å found previously in poly(urethane–ureas).[15] The halo for the unstretched sample possessed an isotropic intensity along its circumference. After being stretched to 700% elongation, the increased intensity on the equator and decreased intensity on the meridian indicate that the chains are highly oriented, but the absence of equatorial spots indicates that stress-crystallization is not occurring. Longer exposure times still did not reveal any equatorial spots, which are clearly visible for poly(urethane–ureas) even at lower elongations.[15] While these results do not definitively rule out the presence of stress crystallization in materials based on higher molecular weight polyols, they do indicate that it is not the sole cause of the strain-hardening behavior and that the finite extensibility of the polyol chains also makes a contribution.

D. Small-Angle X-ray Scattering (SAXS). Small-angle X-ray scattering data for this series of ionomers reveals the "ionomer" X-ray peak as well as a noticeable shoulder at higher scattering angles as discussed previously.[3] We have proposed a morphological model for these materials, shown schematically in Figure 8 of the preceding paper. By fitting the model equations to the SAXS data, we obtain values of the multiplet radius (R_1), the distance between multiplets (D), the micronetwork radius (R_{CA}), and the volume fraction of the micronetworks in the material (V_f). The shell number (SN) was set to unity and the cross-link functionality (CF) was set to eight, based on results given in the preceding paper in this issue. The SAXS parameters obtained from this bead–spring micronetwork model are summarized in Table III. R_1 changes little with either polyol molecular weight or ionization, reflecting little change in the size of the ionic multiplet with ion content of the material. Since the number of the ions in each multiplet is reflected in the cross-link functionality, which has been held constant for all fits of the data, a large change in R_1 would have been unexpected. D increases slightly with polyol molecular weight. This parameter should be related to the size of the polyol coil, which was considered to be Gaussian in development of the model; however, D increases with polyol molecular weight slower than the expected 0.5 power. Moreover, the value of D increases with ionization level, a trend for which we presently have no explanation. The polyol conformation is currently under further examination by small-angle neutron scattering.

Finally, V_f increases with ion content, either upon increasing ionization level or decreasing polyol molecular weight. This is expected, since the presence of more ions in the system naturally leads to a larger volume fraction of ionic clusters. This parallels the trend found by tensile testing and dynamic mechanical analysis, wherein the modulus was found to increase with ionic content. In short, the parameters obtained from the SAXS data by using the bead–spring micronetwork model follow the expected trends based on the physical property data (with the possible exception of the D values), generally supporting the validity of the model.

Conclusions

The effects of polyol molecular weight and ionization level on the structure–property relationships within a family of sulfonated PTMO–MDI polyurethane ionomers were studied. The rubbery plateau modulus was found to depend solely on the fraction of ionic groups in the material. The glass transition temperature was adequately described by the Fox equation for the unionized polyurethanes. As the ionization level increased, the matrix T_g dropped due to aggregation of the ionized MDI units. For the higher soft segment molecular weights studied, soft segment crystallinity was observed at low ionization levels. Increasing the ionization level decreased the crystallite melting temperature and endotherm area, possibly due to restriction of crystallite size by the ionic aggregates. WAXS measurements on a sample prepared from PTMO 668 revealed no stress crystallization, although this phenomenon may be present in ionomers prepared from polyols of higher molecular weight. The SAXS modeling results are generally consistent with the physical property trends obtained from thermal and mechanical measurements.

Acknowledgment. We acknowledge partial support of this research by the Polymers Section of the NSF Division of Materials Research through Grant DMR 86-03839, by the U.S. Department of Energy through Contract DE-ACO2-81-ER10922, and by the Office of Naval Research through Contract N00014-83-K0423. R.A.R. thanks the staff of the Cornell High Energy Synchrotron Source (CHESS) of the Wilson Synchrotron Laboratory at Cornell University for the opportunity to perform the WAXS measurements and thanks S. C. Johnson and Son and the Fannie and John Hertz Foundation for financial support while this work was performed.

References and Notes

(1) Eisenberg, A.; King, M. *Ion Containing Polymers: Physical Properties and Structure*; Academic: New York, 1977.
(2) Macknight, W. J; Earnest, T. R. *J. Macromol. Sci., Rev. Macromol. Chem.* **1981**, *16*, 41.
(3) Lee, D.-c.; Register, R. A.; Yang, C.-z.; Cooper, S. L., preceding paper in this issue.
(4) Fox, T. G. *Bull. Am. Phys. Soc.* **1956**, *1*, 123.
(5) Lee, W. A.; Rutherford, R. A. In *Polymer Handbook*, 2nd ed.; Brandrup, J., Immergut, E. H., Eds.; Wiley: New York, 1975; pp 111–157.
(6) Ward, T. C.; Tobolsky, A. V. *J. Appl. Polym. Sci.* **1967**, *11*, 2403.
(7) Mooney, M. *J. Appl. Phys.* **1940**, *11*, 582.
(8) Rivlin, R. S. *Philos. Trans. R. Soc. London, A* **1948**, *241*, 379.
(9) Mark, J. E. *Rubber* Chem. *Technol.* **1975**, *48*, 495.
(10) Ferry, J. D.; Kan, H.-c. *Rubber Chem. Technol.* **1978**, *51*, 731.
(11) Dossin, L. M.; Graessley, W. W. *Macromolecules* **1979**, *12*, 123.
(12) Flory, P. J. *J. Chem. Phys.* **1947**, *15*, 397.
(13) Mark, J. E. *Polym. Eng. Sci.* **1979**, *19*, 255, 409.
(14) Clough, S. B.; Schneider, N. S. *J. Macromol. Sci., Phys.* **1968**, *2*, 553.
(15) Bonart, R. *J. Macromol. Sci., Phys.* **1968**, *2*, 115.